DESIGN, FABRICATION, DSP IMPLEMENTATION AND COMPARISON OF SIMULATED PERFORMANCE OF A LINEAR INDUCTION MOTOR FOR P-I AND H_∞ CONTROL SCHEMES

Bijoy K. Mukherjee, A.Sengupta, S. Maiti, M. Sengupta
Dept. of Electrical Engg., Bengal Engg. College (D.U.),
Howrah 711103, West Bengal, India
Tel.: +91-033-2668 4561 extn.222/ Fax: +91-033-2668 4564
e-mail: vj_bec@rediffmail.com, aparajitasg@rediffmail.com, sgall@vsnl.net

Key Words

DSP, Field oriented control, LIM fabrication, PI control, Robust control

Abstract

From conveyors to the high-speed MAGLEV vehicles, from knitting machines to the sophisticated robotic systems, Linear Induction Motors (LIMs) have got a wide range of applications. They have got all the potential to replace the age-old belt-pulley driven systems completely in the coming years. In the present work, a flat, single sided, short primary LIM, which can be used as a linear propulsion system, has been designed and the same has been fabricated. Thereafter PI controllers are designed to implement the field oriented control scheme for use in variable speed drives. The whole system is simulated in the SIMULINK environment of MATLAB and the simulation results are shown. Since the PI controllers cannot handle model uncertainties and parameter variation effects, a robust controller has also been designed. Implementation of the whole scheme is to be done using a DSP in TMS320LF2407A platform. Dry run of the programs has already been done. The inverter is under construction.

1 Introduction

The concept of linear motor is there for quite some time and is soon set to revolutionise propulsion and conveyance systems. Till 1960s the main applications of linear motors were confined only to conveyors, textile shuttle propulsion and the likes. The importance of linear motors gained a tremendous boost in 1970s with the upcoming of Magnetic Levitation (MAGLEV) transport systems. The MAGLEV brought with it an evolution in high-speed ground transportation systems. In MAGLEV vehicles, conventional rotary motors cannot be used to convert rotational motion to linear motion (to remove friction and adhesion). Hence the use of linear motors becomes inevitable. Design, modeling, analysis, fabrication and close loop control of LIM drives has generated much interest during the past two decades[2,10].

In the present work, a flat, single sided, short primary linear induction motor has been designed for use in a lab-scale linear propulsion system. Section 2 contains a concise description of the operating principles of an LIM and the steps of design in brief. The motor is fabricated under the guidance of the authors. Fig. 2 and Fig. 3 show the front and end view of the designed motor respectively. Fig. 16 shows the photographs of the fabricated and successfully tested LIM. The design data for the motor is given in Table 2 in the Appendix. Some experimental results are compared with the designed ones in Table 1. In Section 3 a transfer function of the LIM is derived from the block diagram of its field oriented control. A Proportional-Integral (PI) as well as a robust controller is designed on the basis of the transfer function. The responses of the closed loop systems working with the two controllers

reveal the robust controller gives better performance. All the symbols have been separately defined in the Appendix.

2 Operating Principles and Design

From the operational viewpoint, an LIM can be regarded as an unrolled version of a rotary induction motor. Hence, if a rotary induction motor is cut along a line on its periphery parallel to the shaft direction and laid out flat (as shown in Fig.1), an LIM is obtained. In a three phase LIM, a traveling magnetic field is established which induces voltages in the secondary. When the secondary is shorted, a secondary traveling field is established which interacts with the

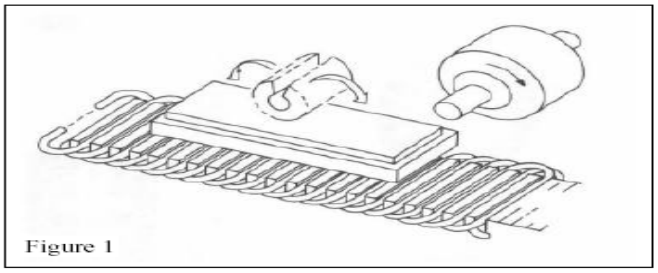

Fig. 1 The concept of Linear Motor

primary field and produces a linear force. Since the primary field induces an opposite pole on the secondary, a normal force, along with the horizontal thrust, is also developed in an LIM. Though from operational point of view, an LIM is very similar to its rotary version, there are some aspects that are peculiar to an LIM only. Some of them will be qualitatively addressed below. The design procedure of an LIM is somewhat different from that of a conventional rotary induction motor. In a conventional motor, both stator and rotor currents are made to flow through guided paths i.e. windings or solid bars. Therefore, the design approach is a circuit approach. In an LIM, on the other hand, the secondary is of distributed nature (being a conducting plate of Al or Cu backed by iron plate). This is why, one has to resort to field theoretical approach for design and analysis of an LIM.

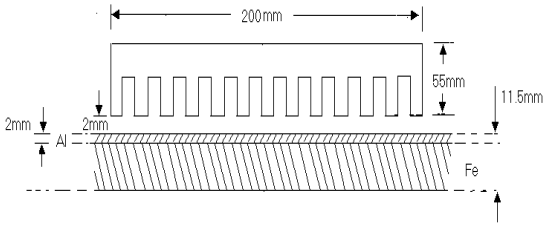

Fig. 2 Front View

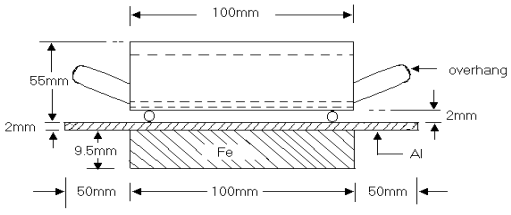

Fig. 3 End View

If supply is given to the stator (primary), then the entire length of the stator is to be laminated, slotted and wound with the polyphase winding. On this count, if the *linor* is the short primary which is excited very long one, the supply can be fed to the linor by a flexible three core cable. Further, for simplicity, a flat, single-sided LIM has been considered. The secondary is made up of a 2mm thick aluminium sheet with a 9.5mm thick steel sheet underneath as shown in Fig. 2 and Fig. 3. The design has been mostly done following [1,2,3] as described below. Synchronous velocity of an LIM is given by, $v_s = 2f\tau$, where, τ is the pole pitch of the machine. The coefficient of friction is taken as 0.4 and the motor is supposed to reach the rated speed within 1 second. To start with it is assumed that the starting force is equal to the rated thrust and is given by, $F_x = \mu mg + mv/t$ and the aluminium track acts as the static secondary, the cost of the machine is less. However, feeding supply to the moving linor (primary) becomes an obvious problem.

The LIM is designed to move a weight of 20 kg at a speed of up to 2.5m/s when operated from a regular 220V, 50Hz, 3-ϕ supply. Now, rated power, $P_m = F_x \times v$. The rest of the design follows the same general procedure as in a conventional induction motor with certain special constraints specific to LIM [1]. For small single-sided LIMs the efficiency-power factor product, ηcosϕ is in the range of 0.1 to 0.4 [1]. For the given thrust, $\eta cos\phi$ is found to be 0.13. In conventional rotary motors, the specific magnetic loading (B_{av}) is chosen in the range of 0.4 to 0.5. However, for LIMs, a lower value is chosen. Also unlike a rotary motor, the voltage drop in the primary is not negligible in an LIM due to higher leakages and longer winding lengths for the end coils. The designed dimensions and other values have been presented in the Appendix. On the basis of the same the LIM was fabricated with the help of local manufacturers at a cost of Indian Rs. 15,000. Table 1 shows a comparison between of some of the designed and experimental parameter values. There is very good agreement showing the accuracy of the design as well as fabrication.

Parameters	Analytical (at slip = 1)	Experimental
R_1	1.40 Ω	1.57 Ω
R_2'	6.13 Ω	6.11 Ω
X_1+x_2'	11.76 Ω	10.49 Ω

Table 1

3 Closed loop control

For different applications of the motor, its speed is to be controlled externally. One simple way of achieving this is by controlling input voltage and frequency maintaining their ratio constant (V/F control). Though the closed loop V/F control yields satisfactory steady state response, it gives poor dynamic response. When applied to linear propulsion systems, good dynamic response and accurate steady state performance are expected from such motor drives. Hence indirect field oriented control scheme is chosen so that the machine can be used as a variable speed drive. The control scheme is simulated using PI controllers and the simulation results are shown. A robust controller is also designed so that the control performance is not adversely affected by parameter variations or disturbances. The simplified block diagram of indirect field oriented control of an LIM is shown in Fig. 4. The same can be implemented by a DSP. The following describes suitable techniques to design the controller blocks marked 'PI'.

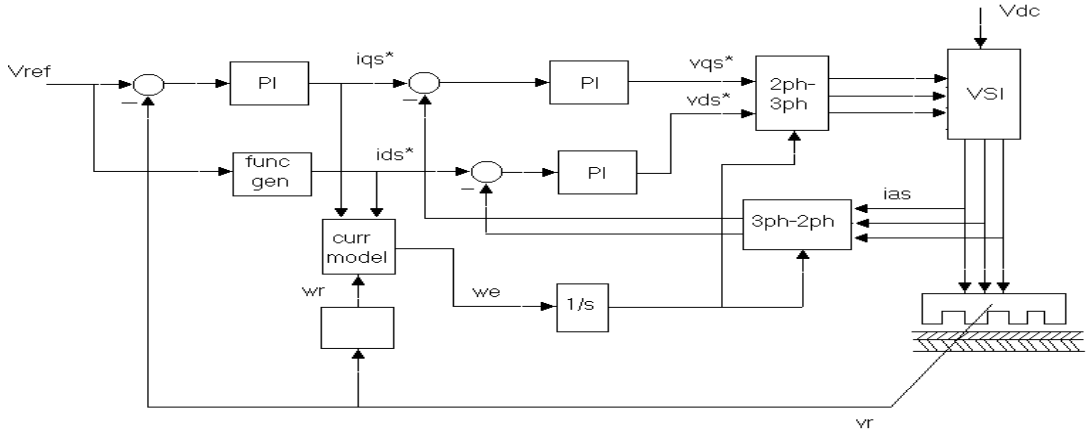

Fig.4 Closed loop control Scheme

3.1 PI Controller Design:

From the d-q equivalent circuit of an induction motor, [4] letting the rotor flux linkage to be aligned along the d axis of the synchronously rotating reference frame,

$v_{qs}(s) = (R_s + sL_a)i_{qs}(s) + \omega_e L_s\, i_{ds}(s)$ (in s domain), substituting, $\omega_e = \omega_r + \frac{1}{T_r}\frac{i_{qs}}{i_{ds}}$ and

rearranging, $i_{qs}(s) = \frac{K_a}{1+sT_a}\left[v_{qs}(s) - \omega_r L_s i_{ds}(s)\right]$ (1)

From the expression of the electromagnetic torque and from the dynamic equation of the motor and neglecting load torque,

$$\frac{\omega_r(s)}{i_{qs}(s)} = \frac{K_m}{sJ} \quad (2)$$

Fig.5 shows the complete block diagram considering (1) and (2) with the speed control loop along with an inner current control loop with classical PI controllers. v_{qs} is supplied from the inverter. In Fig.5, the inverter is shown as a first order transfer function where T_{in} is the time period of the carrier wave. However, as the carrier wave frequency is very high (2250 Hz) [9], T_{in} can be neglected. Therefore, the inverter is considered as an amplifier with a gain given by, $K_{in} = 17.96$.Fig 6. shows the reduced block-diagram of the inner current control loop alone and from it the transfer function G1 is found to be,

$$G1(s) = \frac{387.76s}{s^2 + 128.04s + 2607.2} \quad (3)$$

Allowing a steady state error to unit step input of 2% the current controller is designed to be,

$$K_c = \frac{8.66s + 329.46}{s} \quad (4)$$

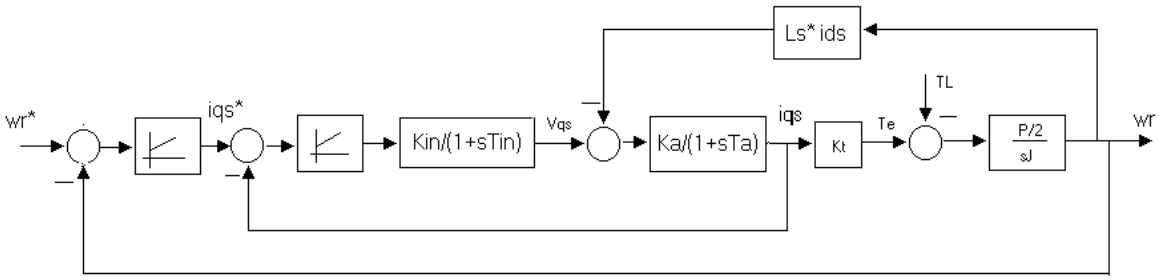

Fig.5 Speed and current control loops

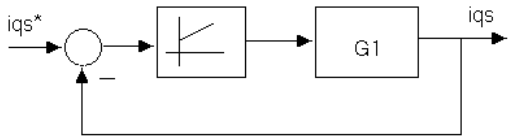

Fig.6 Reduced block diagram of the current control loop

In Fig 4., the speed controller $K_s = \frac{157.25s + 62.9}{s}$ and the flux controller is set at $\frac{9.81s + 174.4}{s}$ is selected by trial and error. The speed response for the nominal plant is shown by the blue trace in Fig. 14.

3.2 Design of Robust Controller using μ Synthesis:

It has been observed that the parameters of the LIM vary considerably with variation in slip. It has been seen that these variations hardly affect the performance of the current control loop but the speed response gets worsened substantially. Here, therefore, we shall design robust controllers for the speed control loop keeping the PI current controller intact. We shall apply both H_∞ synthesis and μ synthesis methods and compare their performances. Keeping the PI current controller as in (4), the reduced block diagram of the speed control loop is shown in Fig.9. The nominal transfer function is given by,

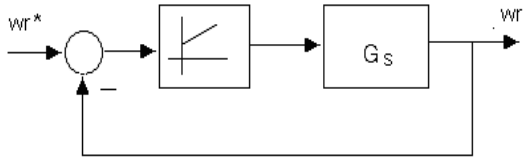

$$G_s(s) \approx \frac{7.08 \times 10^5}{s(s+3448)}$$

Fig. 9 Reduced block diagram of the speed control loop

Considering the variation in slip to be within 0.6 and 0.3 and also considering the change in secondary resistance due to temperature rise to be 30% [6], two perturbed plants are found to be,

$$G_{s1}(s) = \frac{1.78 \times 10^5}{s(s+2884)} \text{ and } G_{s2}(s) = \frac{2.62 \times 10^5}{s(s+3725)}.$$

We shall design the speed controller considering this variation in G_s and taking into account load disturbance neglecting the effect of sensor noise. This is the mixed sensitivity problem. The closed loop interconnection corresponding to this problem is shown in Fig.10.

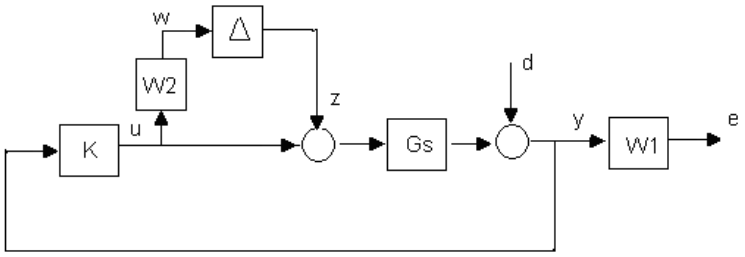

Fig. 10 Interconnection corresponding to mixed sensitivity problem

The uncertainty weight $W_2(s)$ is computed as,

$$W_2(s) = \frac{G_{s1} - G_s}{G_s} = -0.75\frac{s+2698}{s+2884}$$

The sensitivity weight $W_1(s)$ is chosen to be

$W_1(s) = \dfrac{0.4s+500}{s+1}$ corresponding to a steady state error of 0.2% and a settling time of 0.01 sec.

Bode plots of W_1^{-1} and W_2^{-1} are shown in Fig. 11.

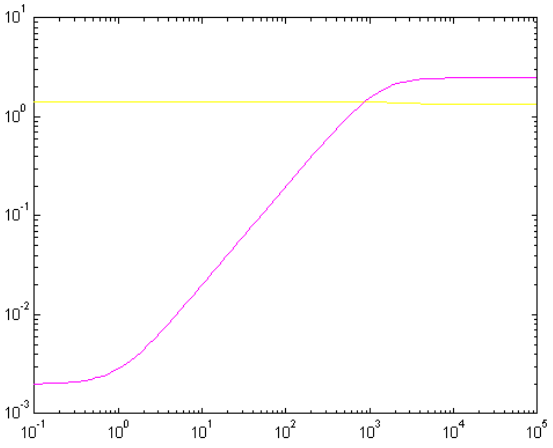

Fig. 11 Plots of W_1^{-1} and W_2^{-1} versus frequency

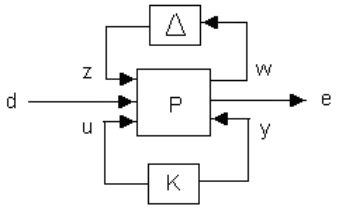

Fig. 12 LFT of Fig.10

The system in Fig. 10 is framed in the LFT framework as shown in Fig 12. The augmented system matrix P is obtained with the help of MATLAB. The perturbation matrix Δ is considered to be a complex scalar block. The augmented system matrix P is supplied to the D-K Iteration Graghical User Interface (dkitgui) of the μ-Analysis and Synthesis toolbox of MATLAB and the robust performance conditions have been found to be satisfied after three iterations. The resulting controller is of 14th order. A reduced 6th order controller has also been obtained using simple pole-zero cancellation method and the corresponding step response is shown in Fig.13. The response of the robust controller (Fig. 14) has been observed to handle the parameter variation effects better than the PI controller does. The robust controller also gives better disturbance rejection.

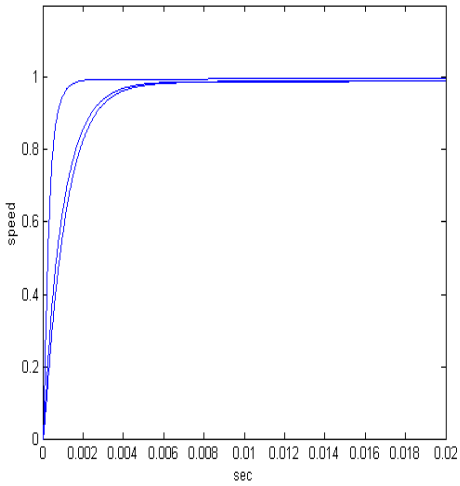

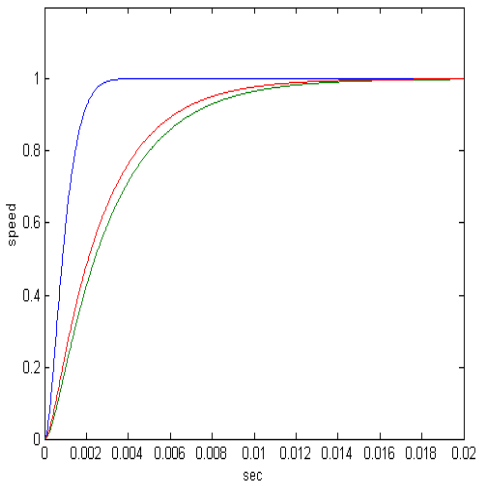

Fig. 13 Speed response 6th order robust controller Fig. 14 Speed Response PI controller

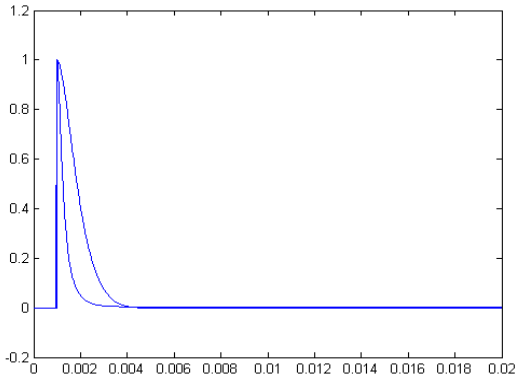

Fig. 15 Output due to unit step disturbance using PI & 6th order robust controller

4 Bibliography

[1] Gieras J.F., "*Linear Induction Drives"*, Oxford University Press, New York, 1993.
[2] George H.Abdou and Sherif A.Sherif, "*Theoretical and Experimental Design of LIM in Automated Manufacturing Systems",* IEEE Trans. on Industry Applications, March/April,1991,pp.286-293.
[3] Sawhney A.K.,*"A Course in Electrical Machine Design"*, Dhanpat Rai & Sons, New Delhi, 1990.
[4] Bose B.K., "*Modern Power Electronics and AC Drives",* Pearson Education, New Delhi, 2002.
[5] Chee-Mun Ong, "*Dynamic Simulation of Electric Machinery Using Matlab/Simulink",* Prentice Hall, New Jersy, 1998.
[6] Krishnan R., "*Electric Motor Drives – Modeling, Analysis and Control",* Prentice-Hall of India, New Delhi,2002.
[7] Zhou K.,and Doyle J.C., "*Essentials of Robust Control"*, Prentice Hall, New Jersy, 1997.
[8] TMS320LF2407A-*User's Guide,* Texas Instruments, 2002.
[9] "*Power System Blockset - Users' Guide*", The MathWorks, Inc., 2001.
[10] Atencia J., Martinez-Iturralde M., Garcia R. A. and Florez J., "*Modeling of Linear Induction Motors as linear drives",* IEEE Conf. On Power Technology, Porto, Portugal, 2001.

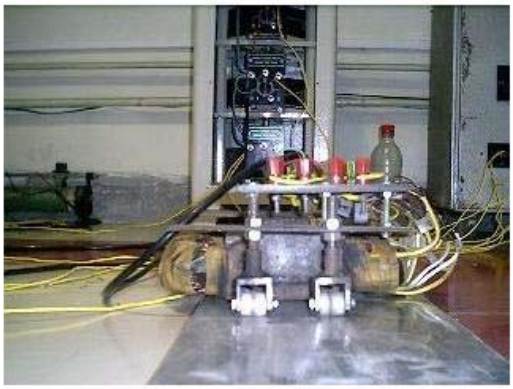

Fig.16 Photographs of the fabricated LIM (a) End view (above) (b) Top view (left).

5 Appendix

List of Principal Symbols:

$K_m = 2.11$ $J = 0.01\ kg=m^2$ $W_1(s)$: Sensitivity weight $W_2(s)$:Uncertainty weight Δ:stable real-rational T.F., $\|\Delta\|_\infty < 1$ d: disturbance y:measured output e: controlled output u: control input	v_{qs}:q-axis supply voltage R_s:primary resistance i_{qs}:q-axis primary current ω_e:synchronous speed L_s:primary inductance i_{ds}:d-axis primary current L_m:mutual inductance i_{dr}:d-axis secondary current $K_a = 1/R_a = 0.1686$ $T_a = L_a/ R_a = 7.81 \times 10^{-3}\ s$

Item	**Value**		**Item**	**Value**
Terminal voltage, V_L	220 V		Slot width, w_{ss}	10 mm
Supply frequency, f	50 Hz		Tooth width, w_{ts}	6.66 mm
No. of primary phase, m_1	3		Slot depth	45 mm
No. of poles, P	4		Depth of back iron, h_{1y}	10 mm
Pole pitch, τ	50 mm		Conductors per slot, z_s	120
Rated linear force, F_x	100N		Bare diameter of conductor, d_0	1.4mm
Rated velocity, v	2.5 m/s		Current density, J_0	4.25 A/mm^2
Synchronous velocity, v_s	5 m/s		Length of overhang, w_{ov} (each side)	50 mm
Rated power, P_m	300 Watt		Length of mean turn, L_{mt}	0.425 m
Full load line current, I_1	6.56 A		Length of air gap, g	2 mm
Specific magnetic loading, B_{av}	0.25 Tesla		Thickness of Aluminium plate, d	2mm
Specific electric loading, A_{my}	66,667 A/m		Width of Aluminium plate	200 mm
Length of primary, $P\tau = \pi D$	200 mm		Thickness of iron plate, h_{sec}	9.5 mm
Width of primary, L_i	100 mm		Width of iron plate, w :	100 mm
Lamination thickness	0.5 mm		Magnetizing current, I_m	2.29A
Type of primary winding	Double layer		Primary resistance (per phase), r_1	1.40 Ω
Connection	Star		Per phase primary leakage reactance, x_1	9.16Ω
Flux per pole, ϕ_m	1.25 mWb		Magnetizing reactance, X_m	28.8Ω
Primary turns per phase, N_1	240		Secondary resistance (per phase) at rated slip, r_2'	4.23Ω
No. of primary slots	12		Secondary leakage reactance (per phase) at rated slip, x_2' :	6.62Ω
Slot per pole per phase, SPP	1		Efficiency at full load, η	0.3
Winding factor, k_w	1		Power factor at full load, cosϕ	0.39
Slot pitch, y_{ss}	16.66 mm			

Table 2 Design data of the LIM